International Journal of Engineering Science Invention (IJESI)
ISSN (Online): 2319-6734, ISSN (Print): 2319-6726
www.ijesi.org ||Volume 10 Issue 6 Series II || June 2021 || PP 01-13

Underwater Image Enhancement Using Teleost Fish Retinal Mechanisms

T. Hema Latha[1], Babu Rao Markapudi[2], Kavitha Chaduvula[3]

[1]*M.Tech Student, Dept. of Computer Science & Engineering, Gudlavalleru Engineering College, Gudlavalleru, Andhra Pradesh, India*

[2] *Professor & Head, Dept. of Computer Science & Engineering, Gudlavalleru Engineering College, Gudlavalleru, Andhra Pradesh, India*

[3]*Professor & Head, Dept. of Information Technology, Gudlavalleru Engineering College, Gudlavalleru, Andhra Pradesh, India*

ABSTRACT: *The main aim of this paper is to solve the issues of blurring and non-uniform color biasing that cause underwater image degradation. To correct the non-uniform color bias, color-sensitive horizontal cells provide input to cones, as well as a red channel compensation. The bipolar cells' center-surround opponent mechanism, as well as input It helps to enhance the output image's edges and contrasts by switching from amacrine cells to interplexiform cells, then to horizontal cells. Color enhancement and correction are carried out by ganglion cells with a color-opponent mechanism. Finally, we use a luminance-based fusion technique to recreate the enhanced image by combining the outputs of the ON and OFF pathways of the fish retina. Our model automatically guides the design of each low-level filter using global statistics (such as image contrast), allowing the main parameters to self-adapt.*

INDEXED WORDS: *Color correction, underwater image processing, biologically inspired vision*

Date of Submission: 02-06-2021 Date of Acceptance: 16-06-2021

I. INTRODUCTION

The following are the major contributions:(i)We model the retinal feedback mechanisms from horizontal cones of color-sensitive cells to create a non-uniform CC processing that can manage non-uniform colour bias in underwater images better than previous state-of-the-art methods (SOTAs), which are typically based on the assumption of uniform colour bias (e.g., grey world assumption). (ii) For colour enhancement and colour correction, a new sharpening operation based on the color-opponent mechanisms of retinal ganglion cells is suggested, which is very versatile in terms of adjusting the colour appearance of underwater images. (iii) The center-surround opponent mechanisms of bipolar cells are used for flexibly filtering out the low-pass and band-pass frequencies of underwater images, which can effectively transfer the edge and contrast information to the output. (iv) Each low-level filter's primary model parameters transform in response to the input image's global contrast, visualising the dynamic modulation of the nearby region to the central part of a neuron's receptive field (RF).

Fig 1: original under water image

ALGORITHMS FOR IMAGE ENHANCEMENT

a. Medical image enhancement techniques algorithm:

The results of enhancing electron microscopy, radiological, CT scan, and MRI scan images using the MATLAB environment are compared to the original images as well as other enhancement approaches such as contrast enhancement and two forms of adaptive contrast enhancement.

b. An improved de-noising algorithm for fractal images:

Using a quadratic gray-level function, An improved fractal predictive de-noising algorithm for de-noising images corrupted by additive white Gaussian noise is described in this paper (AWGN). Meanwhile, to strictly guarantee the enhanced fractal codling's contractively requirement, a quantization method for the quadratic function's fractal gray-level coefficients is proposed, and in terms of the accuracy of the fractal representation defined by PSNR, In the vast majority of instances, enhanced fractal image coding with quadratic gray-level function outperforms standard fractal image coding with linear gray-level function.

c. Algorithms for improving funds images analysis:

The occurrence of noise and light objects in retinal colour images is unavoidable.

It's preferable to homogenise non-uniform illumination and increase contrast while retaining colour characteristics in order to enhance the diagnostic quality of the images. Different pre-processing techniques can produce very different visual effects, so it's crucial to test them critically before determining which is best. The output of eight algorithms for correcting non-uniform illumination, adjusting contrast, and maintaining colour was evaluated in this article. A general evaluation was presented in order to select the most acceptable.

Two new automated image processing algorithms for contrast enhancement of portal images are provided as appropriate tools for setup verification and visualisation of patients during radiotherapy treatments. In the first algorithm, Automatic Segmentation and Histogram Stretching, the portal image is automatically segmented into two sub-images delimited by the conformed treatment beam (ASHS).

These two algorithms have been tested on a variety of portal images and have yielded excellent results.- Highlights: To enhance contrast of Electronic Portal Images, two algorithms are used. Portal Images are automatically segmented from the multi-leaf and conformed beam. Portal images show concealed anatomical and bony structures. The job of checking the patient setup is made simpler by the contrast enhancement that is achieved.

d. Underwater Image Enhancement Algorithms are Implemented in a Multitude of Environments:

There is a full text version available. Because of light scattering and absorption, underwater photographs usually have low visibility, loss of contrast, and colour casting. Many algorithms exist in the literature that strive to improve the quality of underwater images using various approaches.Our goal was to find an algorithm that could perform well in a variety of environments. We chose some state-of-the-art algorithms and used them to improve a dataset of photographs taken in a variety of underwater locations, each with its own collection of environmental and lighting conditions. Quantitative metrics were used to assess these enhanced images. We tried to figure out which of the chosen algorithms performed better than the others by analysing the effects of these metrics.

PROBLEM STATEMENT:

As stated earlier, image processing analysis poses some challenges, especially in the context of underwater image enhancement. It has been noted that researchers in the field of marine exploration in general, and computer science in particular, are having trouble obtaining high-quality underwater images. Such issues must be resolved in order to conduct through and accurate study of underwater objects. Most significantly, the issues must be resolved during the computer vision system's pre-processing stage. The issue of image enhancement is becoming increasingly important, given the theoretical and technical perceptions of marine science.

This approach presents one of the most important issues: how to enhance the accuracy of underwater images in order to streamline image processing analysis.

II. LITERATURE SURVEY-

"R. Schettini and S. Corchs":

The field of underwater image processing has gotten a lot of attention in recent decades, and it has made tremendous progress. In this article, we look at some of the most recent underwater approaches that have been developed specifically for the region. These techniques can improve image contrast and quality while also expanding the range of underwater photography. After reviewing the fundamental physics of light propagation in the water medium, we focus on the various algorithms available in the literature. The circumstances in which they were made, as well as the quality assessment methods used to assess their performance, are highlighted. The image processing group faces a challenge in achieving illumination of objects in underwater scenes at long or short distances. Even though there are numerous image enhancement techniques available, they are mostly limited to ordinary images, and only a few have been created specifically for underwater images. We've looked at a few of them in this article with the aim of putting the details together for a better understanding and comparison of the approaches. We've compiled a list of available image restoration and enhancement techniques, concentrating on the conditions for which each algorithm was originally built. We also looked at the methods used to assess the algorithms' results, highlighting the papers that used a quantitative quality metric.

"A. T. Olmos-Antillon and E. Trucco":

On the basis of a simplified version of the Jaffe–Mc Glamery underwater image formation model, a self-tuning image restoration filter is presented. By optimising a quality criterion based on a global contrast metric, optimal values of the filter parameters are generated automatically for each individual image. Although the simplified model is best for diffuse-light imaging with low backscatter, qualitative tests show that it performs well in a variety of imaging scenarios. Furthermore, quantitative experiments using a large number of frames from six actual mission videos show that using restoration as a pre-processor for a classifier detecting man-made objects in unconstrained subsea videos improves performance significantly. A self-tuning restoration filter based on a simplification of the general Jaffe – Mc Glamery underwater image forming model, as well as a succinct account of the latter, has been presented in this paper. The simplified model is best suited to shallow-water, diffuse-light conditions with low backscatter, but experimental results show that it can be useful in a variety of imaging situations. In the sense that optimal parameter values are calculated for each image, the algorithm presented is self-tuning. The Tenengrad criterion defines optimality as achieving the least amount of blur. Quantitative tests using a large number of frames from real-mission videos show a significant, quantitative increase in detecting man-made objects on the sea floor, a critical classification task for subsea operations.

"G. Kervern, J.-P. Malkasse, and A. Arnold-Bos":

The light absorption and scattering by the marine environment, which restricts visibility distances to a few miles in coastal waters while using low-end cameras, is a major impediment to underwater operations using cameras. We suggest a comprehensive pre-processing system capable of dealing with the full range of noises found in underwater videos. We show that the majority, if not all, of this pre-processing can be achieved with very generic methods that don't involve any awareness of the scene or the water's turbidity characteristics while staying consistent with the underwater image forming model.

"S. Bazeille, I. Quidde, L. Jaulin, and J.-P. Malkasse":

For underwater image restoration, a novel pre-processing filter is proposed. Due to the unique transmitting properties of light in water, underwater images have a restricted range, uneven illumination, poor contrast, reduced colour, and significant blur. Today's pre-processing methods normally focus on non-uniform lighting or colour correction, and they often necessitate additional environmental awareness. The algorithm proposed in this paper is an automated underwater image pre-processing algorithm. It increases image quality and eliminates underwater perturbations. It is made up of several independent processing steps that correct uneven lighting, suppress noise, improve contrast, and change colours. A robustness criterion for edge detection will be used to evaluate filtering efficiency.

"H. Lu, Y. Li, and S. Serikawa"

By using directed trigonometric bilateral filters and colour correction, this paper describes a novel method for improving underwater optical images. For underwater optical photography, scattering and colour distortion are two main causes of distortion. Large suspended particles, such as fog or turbid water with a lot of particles, cause scattering. Colour distortion is caused by the varying degrees of attenuation experienced by light travelling in water with various wavelengths, resulting in a bluish tone in ambient underwater environments. Proposing a new underwater model to compensate for attenuation differences along the propagation path, as well as a quick directed trigonometric bilateral filtering enhancing algorithm and a novel fast automatic colour enhancement algorithm, are among our major contributions. Reduced noise, better dark region visibility, and improved global contrast classify the enhanced images, while fine details and edges are dramatically improved. Furthermore, by assuming in the most recent image assessment systems, our enhancement approach is comparable to higher quality than state-of-the-art methods.

III. PROPOSED METHOD

3.1 THE FISH RETINA INSPIRED MODEL

As shown in Fig. , our model follows the basic visual signal processing mechanisms in the teleost fish retina.

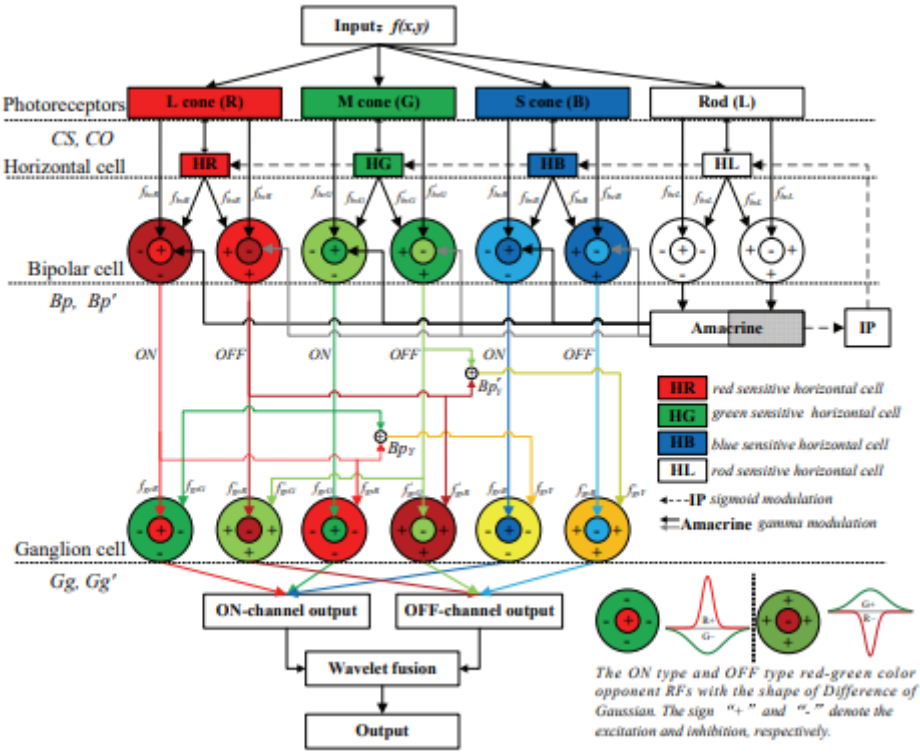

Fig 2: The block diagram of the model proposed by the retinal mechanisms of fish.

1. Photoreceptors

The images can be classified into the rod and cone types, as the first layer of the retina, which is used for transmitting the received light to the neural response. Cone cells could be further separated in long (R), middle (G), and short (B), depending on their sensitivity to the wavelength of the spectrum[60].Our underwater f(x,y) channels are separated into R, G and B channels and treated as cone cell inserts. The lighting signal received by rod cells are simply defined as

$$L(x,y) = (f_R(x,y) + f_G(x,y) + f_B(x,y))/3 \quad (2)$$

2. Horizontal cells

Horizontal cells (HCs) have the largest RF size in the retina, enabling them to integrate photoreceptor signals over relatively large areas. The first feedback path in the retina (e.g., the bidirectional arrow between photoreceptors and HCs shown in Fig. 2), which is key to the realisation of CC, is from HCs to photoreceptors.

The global mean of each of the R, G, and B channels is used as the feedback of HCs to each cone type in existing CC models influenced by retina mechanisms [1], which obviously ignores the non uniform colour variation of the underwater world. Furthermore, interplexiform cells have an inhibitory regulation on horizontal cells, which is not taken into account by most retinal models. To simulate the RF of HCs in our model, we use a

local mean filter, which estimates the local light source colours from the input and then returns the estimated local signal as feedback to correct the signal encoded by the cone cells.

Since fish eyes are more susceptible to longer wavelength lights [2], [3], [4], [5], and the red portion of an underwater object is usually much weaker than the blue and green components, HC feedbacks in the red channel are measured globally using the bright sections of the scene to avoid red artifacts after CC processing. In each of the three channels, the HC feedbacks are determined as follows:

$$HCF_R(x,y) = \underset{f_R > 0}{mean}\{\{f_R(x,y)\}mean_{N\times N}\}$$
$$HCF_G(x,y) = \{f_G(x,y)\}mean_{N\times N}(3)$$
$$HCF_B(x,y) = \{f_B(x,y)\}mean_{N\times N}$$

Where is a parameter that controls the selection of the red channel's bright sections. When there is no pixel value higher than in the local window fR NN centred at, we set HCF R(x, y) = max (fR NN) to monitor the selection (x, y). The approximate light source colour map returned by HC feedbacks (i.e., HCF(x, y), R, G, B) varies significantly from two methods widely used for CC processing of an underwater image [6], [7].

Since the colour modulation within an underwater picture is rarely spectrally uniform, our proposed HC feedbacks estimate a spatially varying light source colour map, which is very useful for non uniform CC [8]. The traditional approaches, on the other hand, often return a standardised light source colour m.

$$CS_\lambda(x,y) = \frac{f_\lambda(x,y)}{HCF_\lambda(x,y)}, \lambda \in \{R,G,B\}(4)$$

The interplexiform cells then release dopamine to inhibit horizontal cell operation in a dark environment, thereby improving the contrast of image components with intermediate brightness [9], [10]. As a result, after being modulated by HC feedbacks, we use the sigmoid function to suppress the dim part of cone signals, and the final cone signals are

$$CO_\lambda(x,y) = \frac{1}{1+e^{-10(CS_\lambda(x,y)-0.5)}}, \lambda \in \{R,G,B\}(5)$$

Except that the rod pathway has only one channel (i.e., L), we can easily get the output of rod cells COrod(x, y) using Esq. (3) (5) with the input L(x, y). Finally, the modulated signals (CO(x, y) and COrod(x, y) are sent to the layer of bipolar cells with the spatial core surround RF to enhance the contrasts and edges locally.

Bipolar Cells:

The layer of bipolar cells divides the visual signal processing in the retina into ON and OFF pathways. Furthermore, through amacrine cells, bipolar cells on rod pathways can excite or inhibit bipolar cells on cone pathways. As a result, the RF core of bipolar cells on cone pathways receives feedback from amacrine cells as well (as indicated by the black and grey arrows from the amacrine cells to bipolar cells in Fig. 1). A two-dimensional Gaussian function is defined as:

$$g_\sigma(x,y) = \frac{1}{2\pi\sigma^2}\exp(\frac{-x^2+y^2}{2\sigma^2})(6)$$

By convolving the cone signals with a Difference of Gaussian (DOG) function, the response of bipolar cells could be determined as follows:

Bp(x; y)=max[0; (fbc g_c) (x; y) □k_(fbs g_s) (x; y)] Bp(x; y)=max[0; (fbc g_c) (x; y) □k_(fbs g_s) (x; y)] (7)

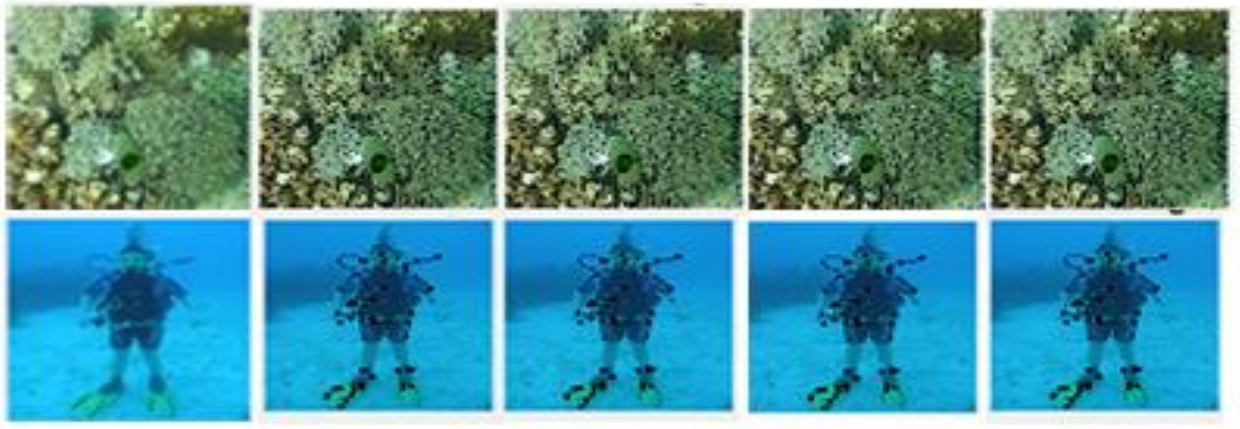

(a) (b) (c) (d) (e)

Fig: CC with various values of θ. (a)original images, (b) $\theta = 0.3$ (c) $\theta = 0.15$ (d) $\theta = 0.25$ (e) $\theta = 0.45$.images with global contrast improvement.

The convolution process is indicated by the letters Bp and Bp0, which denote the outputs of ON and OFF bipolar cells, respectively. ON bipolar cells' central and surround RF inputs are denoted by fbc and fbs. The inputs to the central and surround RF of OFF bipolar cells are f0bc and f0bs (see Eqs. 10)(12) for computation). fbcL and fbsL are the signals of rod cells and the signals of rod cells after modulation by the rod horizontal cells, respectively, for the rod pathway of bipolar cells:

$$f_{bcL} = CO_{rod}(x, y)$$
$$f_{bsL} = \{CO_{rod}(x, y)\} mean_{N \times N} (8)$$

Similarly, we can compute the output of rod bipolar cells as:

$$0, (f_{bcL} \otimes g_{\sigma_c}(x, y) - k * (f_{bsL} \otimes g_{\sigma_s})(x, y)] (9)$$
$$B_{P_{rod}} = max$$

There are two types of inputs for bipolar cells' cone pathway. One input comes directly from the cones, while the other is modulated by amacrine cells and comes from the rod bipolar cells. To simulate the nonlinear modulation of amacrine cells, we use the gamma correction; thus, the input to the RF centre of cone bipolar cells fbc is given by

$$f_{bc}(x, y) = CO_{\lambda}(x, y) * B_{p_{rod}}^{\gamma} (10)$$

In this analysis, we set the value to 0.5 as an experiment. Fbs is the cone signal that is locally processed by horizontal cells and then fed into the RF surround of cone bipolar cells.

$$f_{bs}(x, y) = \{CO_{\lambda}(x, y)\} mean_{N \times N} (11)$$

Finally, the signals along the OFF pathways f 0 bc and f 0 bs can be obtained easily using

$$f'_{bc} = 1 - f_{bc}$$
$$f'_{bs} = 1 - f_{bs} (12)$$

The parameters c, s, and k must be defined in Eqs (7) and (9). The DOG's central and surrounding scales are c and s, respectively, and help to minimise picture blurriness. Based on physiological observations, s is usually limited to the three periods of c [11]. Extensive testing showed that when c is set between 0.2 and 0.5 for most underwater images, the processed images by DOG are transparent and insensitive to this parameter, so we still use c = 0.3 in this job. K is a weight that governs the RF surround's inhibition of the RF core.

Ganglion Cells:

In the fish visual system, the number and types of ganglion cells processing red and green components are much greater than those processing blue components [12], [13], [14]. The ganglion's fine processing of red and green components may be an adaptation to the bluish underwater environments. To increase the colour contrast of images, we selected single opponent cells with red-green and blue-yellow colour opponent mechanisms to make the final enhanced images more appropriate to the senses of the human visual system [15]. The signals from the bipolar cells are received by the RF centre and surround of ON and OFF ganglion cells (i.e., Bp and Bp0), with the red center/green surround, green center/red surround, blue center/black surround, and yellow center/blue surround, this is the RF of ganglion cells (Fig. 2). The yellow channel signals are equivalent to the average of the red and green channel signals from bipolar cells [16], which is calculated as:

$$B_{P_Y} = (B_{P_R} + B_{P_B})/2$$
$$B_{P'_Y} = (B_{P'_R} + B_{P'_B})/2 \ (13)$$

Finally, using a new DOG operation with the colour opponency (DOGCO), the responses of ganglion cells are measured.

$$G_g(x,y) = max\ [0, (f_{gc} \otimes g_{\sigma c} + m * (f_{g_c} \otimes g_{\sigma_c} - f_{g_s} \otimes g_{\sigma_s}))(x,y)]$$
$$'(x,y) = max[0, (f'_{gc} \otimes g\sigma_c + m * (f'_{gc} \otimes g\sigma_c - f'_{gs} \otimes g_{\sigma s})))(x,y)(14)$$

Gg and Gg0 denote the outputs of ON and OFF ganglion cells, respectively, and fgc, fgs, f 0 gc, and f 0 gs denote the signals from bipolar cells (i.e., Bp and Bp0). For example, in ON-type ganglion cells with a red core and a green surround (Fig. 1), the central RF receives the red component of Bp as input fgc, while the surrounding RF receives the green component of Bp as input fgs. Similarly, for the OFF-type ganglion cells with the red center/green surround mechanisms, its central RF takes the red component of Bp0 as the input f 0 gc, while its surrounding RF takes the green component of Bp0 as the input f 0 gs.

Adaptive neural pathways are used to automatically set the parameters k and m.

A DOG mechanism is used to model certain interactions between the RF core and surround of bipolar cells and ganglion cells in Eqs (7) and (14). DOG's efficiency in moving edges and colour contrast, on the other hand, is dependent on the required weights of the RF surround (i.e., k and m), which are difficult to tune automatically. Fortunately, a solution has already been discovered in the mammalian visual system in the form of complex, contrast-based, centre surround cortical interactions [17], [18], which are not included in the HVS-inspired formulations [1], [19], [20]. For example, the effect of the surrounding RF on the central RF varies depending on the local contrast of both the centre and the surround, with higher contrast stimuli causing more inhibition [17]. Although the ultimate function of these non-linear interactions is unknown, we hypothesise that they could be involved in colour and contrast enhancement, and thus suggest an adaptive model that eliminates the need for ad-hoc or dataset-dependent parameters (and in this sense, it is fully automatic).

When the blurriness of an underwater picture is high, which correlates to low contrast stimuli, a larger k calls more surrounding RF signals to increase the local contrast [21]. The density of haze inside underwater images is positively associated with the parameter k, according to our findings.

We directly estimate the dense of haze in the image using DCP [22], which is used as a measure to automatically set the parameter k, since the dense of haze can serve as an indicator for coding the contrast of an underwater image (e.g., higher dense of haze corresponds to lower contrast of image). The average density of haze is approximately proportional to the values of k. t(x, y) in Eq. (1) can be written as follows using the DCP model:

$$t(x,y) = 1 - \min_{x,y \in \Omega}(\min_{\lambda} \frac{I_\lambda(x,y)}{A_\lambda(x,y)}), \lambda \in \{R,G,B\}(15)$$

What is the location of a square patch centred at (x, y). As the calculated non uniform light source colour map, we estimate the background light A(x, y).

$$A_\lambda(x,y) = HCF_\lambda(x,y), \lambda \in \{R,G,B\}(16)$$

In comparison to Eq., the background light A(x, y) is heterogeneous (1). As a result, unlike the widely held assumption in DCP-based dehazing [23], the approximate transmission t(x, y) is color-dependent in space. We will quantitatively show that our proposed non uniform light source colour map will help provide better depth estimation [25] [26] than that of the homogeneous background light because correct depth estimation requires both the background light and the transmission of an underwater image to be correctly calculated [24]. Finally, the value of k can be determined easily using the image's estimated haze as follows:

$$k = mean(\min_{x,y \in \Omega}(\min_{\lambda} \frac{I_\lambda(x,y)}{A_\lambda(x,y)}))(17)$$

That the image's saturation may be viewed as a simple calculation of the image's colour contrast [25] can be used to determine the saturation of an image.

$$S(x,y) = 1 - \frac{3min\ (B_{P_R}, B_{P_G}, B_{P_B})}{B_{P_R} + B_{P_G} + B_{P_B}}(18)$$

We take the average of the second term in Eq. (18) over the whole image as the value of m:

$$m = mean(\frac{3min(B_{P_R}, B_{P_G}, B_{P_B})}{B_{P_R} + B_{P_G} + B_{P_B}})(19)$$

Fusion of ON and OFF Channels:

To fuse the signals from ON-type and OFF-type ganglion cells, we simply use a weighted wavelet process. The aim is to get the benefits of both channels together. Furthermore, during wavelet fusion, potential artefacts due to oversaturated regions of each channel can be minimised.

$$output(x,y) = wavelet\{\omega_{ON}(x,y) * G_g(x,y) + \omega_{OFF}(x,y) *\ \ '(x,y)\}2(20)$$

The weights w ON and w OF F control the contributions of the signals from the OFF and ON channels, respectively. A sigmoid feature is used to emphasise the weight of bright parts of images while weakening the weight of dark parts of images.

$$(x, y) = \frac{1}{1 + e^{-10((x,y)-0.5)}} (21)$$
$$F$$

The normalized weight of the ON pathway i

$$\omega_{ON}(x, y) = \frac{F((x, y))}{(x, y) + F((x, y))} (22)$$

And the weight of the OFF pathway is

$$\omega_{OFF}(x, y) = 1 - \omega_{ON}(x, y) (23)$$

Other fusion-based methods [9], [14], which use various weights to highlight particular regions, differ from our fusion of the luminance information processed by the ON and OFF pathways using Eq. (20). (e.g., Laplacian contrast weight, saliency weight, saturation weight).

LAPLACIAN:

The Laplacian is a two-dimensional isotropic measure of the second spatial derivative of an image. Since it highlights regions of rapid intensity change, the Laplacian of an image is often used for edge detection (see zero crossing edge detectors). The two variants will be discussed together since the Laplacian is often applied to a picture that has already been smoothed with something like a Gaussian smoothing filter to reduce its sensitivity to noise. The operator usually takes one gray-level image as input and outputs another gray-level image.The Laplacian *L(x ,y)* of a pixel-intensified image values *I(x, y)* is given by:

$$L(x, y) = \partial^2 I/\partial x^2 + \partial^2 I/\partial y^2$$

This can be measured with a convolution filter. Since the input image is described as a set of discrete pixels, we need to find a discrete convolution kernel that can approximate the second derivatives in the Laplacian definition. The 2-D LoG function has the form with Gaussian standard deviation and zero centre.

$$LoG(x, y) = -\frac{1}{\pi\sigma^4}\left[1 - \frac{x^2 + y^2}{2\sigma^2}\right] e^{-\frac{x^2+y^2}{2\sigma^2}}$$

In this we process the two step Laplacian operation Laplacian image as follows:

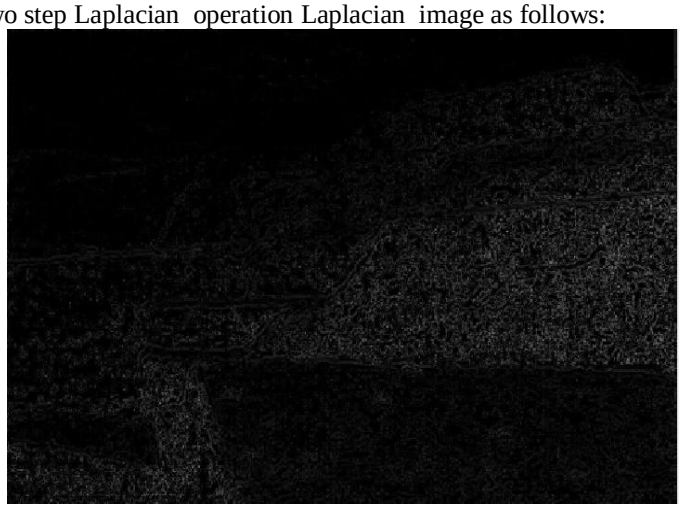

FIG: first step of laplacian level output

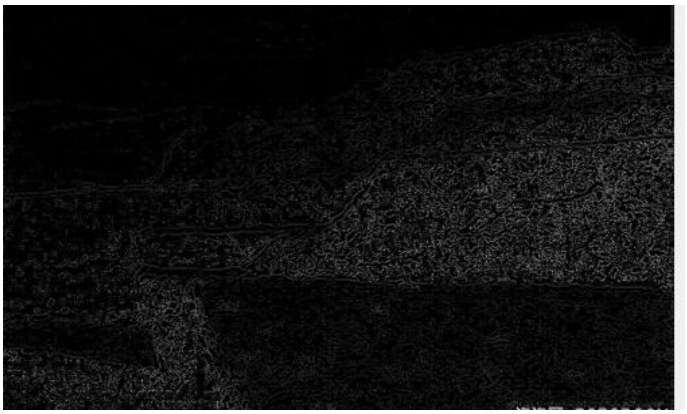

FIG: second step of laplacian level output

SALIENCY DETECTION:

A saliency map is a computer vision image that shows the specific quality of each pixel. In a color image, for example, if a pixel has a high grey level or other specific color quality, that pixel's quality will be visible in the saliency chart. Picture segmentation is a form of saliency.

A saliency map is an image in computer vision that depicts the quality of each pixel. A saliency map's purpose is to make an image's representation more meaningful and easier to analyses by simplifying and/or changing it. For instance, if a pixel in a color image has a high grey level or other distinct color quality, that pixel's quality would be noticeable in the saliency chart. Picture segmentation is known as saliency.

The weighted average of all Gaussian distributions is represented by the Gaussian weight mapping,(G_{pi}) and different saliency preferences are assigned based on the weight distribution difference. As a result, they can refine the saliency mapping by combining the fusion feature mapping and Gaussian weight mapping to produce a visually prominent saliency chart(S_{pi}).

$$S(_{pi})=D(_{pi}).G(_{pi})$$

In this we process the two step saliency operation saliency image as follows:

FIG: first step of saliency level output

FIG: second step of saliency level output

STARTUATION:

The sum of grey in proportion to the hue is represented by saturation, which is the color's intensity or purity. A "saturated" colour is pure, while a "unsaturated" colour contains a lot of grey. To adjust the saturation of each bar, pass the cursor vertically over it.

The comparison of shade determines the value, which is defined as the lightness and darkness of a colour. Although saturation refers to the color's intensity, the addition of grey will reduce saturation.

Saturation occurs when pixels are filled to the point that photons begin to "spill" over the edges. When a pixel accumulates more than 60,000 counts, it is said to be saturated. This is why you should always keep your picture counts between 600 and 60,000.

Image saturation is a term used to characterise the purity or strength of colour in a photograph, so that a photograph with low saturation resembles a black-and-white photograph. Pink is less saturated than red because the red absolutely dominates all colour components in a pure red colour, while grey hues are de-saturated because all colour components contribute equally to the hue.

In this we process the two step saturation operation saturation image as follows:

Fig: At first Step of saturation level output

Fig: second step of saturation level output

(a) (b) (c) (d) (e)

Fig: Calculate the exposedness weight foe saturation The influence of parameters setting on the appearance of processing images the images shows variation among different sigma values

(a). Original image (b). Sigma value=0.5 (c) sigma value=0.15 (d) sigma value=0.25
(e) sigma value =0.45

IV. RESULTS:

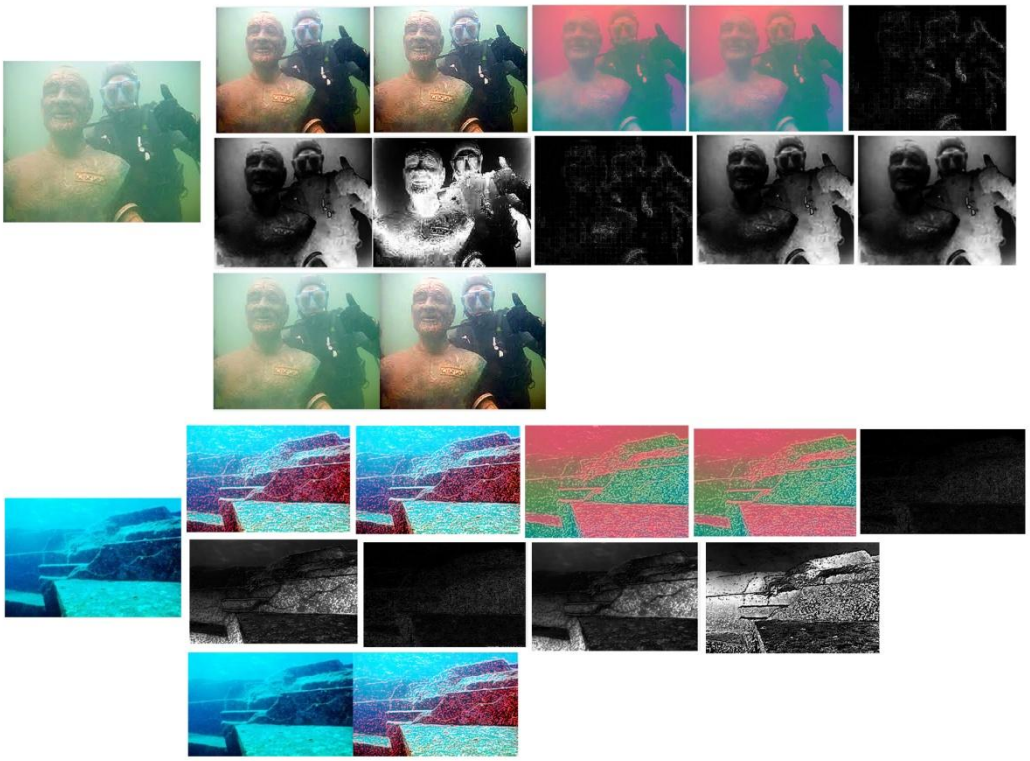

Fig: The results of various under water images with uniform colour bais image enhanced and fusion based methods using various weights (e.g., Laplacian contrast weight, saliency weight, saturation weight). Taking the first image as source image the first column shows the originalthe second to last columns list the corrected images and the corresponding estimated light source colorsand last row image each image shows source image vs output image.

COMPARISIONS:

THE MEASURE OF UC, UQ, MPCQI ON MULTIPLE IMAGES FOR EXISTING METHOD :

NAME OF THE IMAGE	ACCURACY VALUES OF UC	ACCURACY VALUES OF UQ	ACCURACY VALUES OF MPCQI
ship bolt	0.1883	1.0142	0.9592
grey-nurse-sand-tiger-ragged-tooth-shark	0.3666	0.8981	0.4385
coral reef1	0.0481	0.6990	0.9899
Driver1	0.5560	0.4840	0.9246
coral reef2	0.6580	0.3234	0.9601
Driver2	0.4969	2.2594	0.9275
coreel leaves3	0.7822	0.7170	0.9716

THE MEASURE OF UC, UQ, MPCQI ON MULTIPLE IMAGES FOR PROPOSED METHOD:

NAME OF THE IMAGE	ACCURACY VALUES OF UC	ACCURACY VALUES OF UQ	ACCURACY VALUES OF MPCQI
ship bolt	0.6351	0.8126	1.1028
grey-nurse-sand-tiger-ragged-tooth-shark	0.7919	0.1432	1.2029
coral reef1	0.7529	0.2661	1.3484
Driver1	0.5008	0.9586	1.1708
coral reef2	0.8147	0.5911	1.2603
Driver2	0.6932	0.4469	1.0917
coreel leaves3	0.7817	1.1308	1.1891

V. CONCLUSION:

In this work, we proposed a new underwater image enhancement model by carefully considering the features and step by step each in detailed by using image enhancement measurements of the underwater environments and the adaptive mechanisms of the teleost fish retina. Extensive experiments on different underwater datasets show that our method can simultaneously eliminate the haze and the non uniform color bias. Compared to the SOTAs, our technique produces very competitive performance in terms of both qualitative and quantitative evaluations. Moreover, for the first time, we demonstrate the values of modelling the visual mechanisms of underwater creatures for the challenging underwater image processing tasks [1], [24]. We attribute the promising results of this work to the following differences between this work and other existing methods for underwater image processing. i) We introduced a non uniform color correction algorithm, which could well handle the non uniform color cast in underwater images compared to the existing methods that were usually built on the uniform color cast condition. ii) We imitated the adaptive retinal mechanisms to control the model parameters of each low-level filter according to the global contrast of a given image, which overcomes the need for ad-hoc or dataset-dependent parameters (and in this sense, it is fully automatic). iii) We exploited the color-opponent mechanisms to flexibly adjust the color appearance of underwater images during image enhancement. iv) Our algorithm introduced the complementary fusion of luminance information given by the ON and OFF pathways of the retina, which is different from those fusion based methods using various weights (e.g., Laplacian contrast weight, saliency weight, saturation weight).

REFERENCES:

[1]. X.-S. Zhang, S.-B. Gao, R.-X. Li, X.-Y. Du, C.-Y. Li, and Y.-J.Li, "A retinal mechanism inspired color constancy model," IEEE Transactions on Image Processing, vol. 25, no. 3, pp. 1219–1232, 2016.

[2]. R. Douglas and M. Djamgoz, The visual system of fish. Springer Science & Business Media, 2012.

[3]. J. E. Dowling, "Dopamine: a retinal neuromodulator?" Trends in Neurosciences, vol. 9, pp. 236–240, 1986.

[4]. J. N. Lythgoe, Ecology of vision. Clarendon Press, 1979.

[5]. J. Lythgoe, "Visual pigments and environmental light," Vision research, vol. 24, no. 11, pp. 1539–1550, 1984.

[6]. C. Ancuti, C. O. Ancuti, T. Haber, and P. Bekaert, "Enhancing underwater images and videos by fusion," in Computer Vision and Pattern Recognition (CVPR), 2012 IEEE Conference on. IEEE, 2012, pp. 81–88.

[7]. J. Van De Weijer, T. Gevers, and A. Gijsenij, "Edge-based color constancy," IEEE Transactions on image processing, vol. 16, no. 9, pp. 2207–2214, 2007.

[8]. D. Berman, T. Treibitz, and S. Avidan, "Diving into hazelines: Color restoration of underwater images," in Proc. British Machine Vision Conference (BMVC), vol. 1, no. 2, 2017.

[9]. S. Mangel and J. Dowling, "The interplexiform-horizontal cell system of the fish retina: effects of dopamine, light stimulation and time in the dark," Proceedings of the Royal Society of London B: Biological Sciences, vol. 231, no. 1262, pp. 91–121, 1987.

[10]. J. Dowling and B. Ehinger, "The interplexiform cell system. i. synapses of the dopaminergic neurons of the goldfish retina," Proceedings of the Royal Society of London B: Biological Sciences, vol. 201, no. 1142, pp. 7–26, 1978.

[11]. R. Shapley and M. J. Hawken, "Color in the cortex: single-and double-opponent cells," Vision research, vol. 51, no. 7, pp. 701–717, 2011

[12]. N. W. Daw, "Colour-coded ganglion cells in the goldfish retina: extension of their receptive fields by means of new stimuli," The Journal of Physiology, vol. 197, no. 3, p. 567, 1968.

[13]. H. Spekreijse, H. G. Wagner, and M. L. Wolbarsht, "Spectral and spatial coding of ganglion cell responses in goldfish retina." Journal of Neurophysiology, 1972.

[14]. N. Daw, "Neurophysiology of color vision," Physiol. Rev, vol. 53, no. 3, pp. 571–611, 1973.

[15]. K. T. Mullen, "The contrast sensitivity of human colour vision to red-green and blue-yellow chromatic gratings." The Journal of physiology, vol. 359, no. 1, pp. 381–400, 1985.

[16]. D. M. Dacey, B. B. Lee et al., "The'blue-on'opponent pathway in primate retina originates from a distinct bistratified ganglion cell type," Nature, vol. 367, no. 6465, pp. 731–735, 1994.

[17]. A. Angelucci and S. Shushruth, "Beyond the classical receptive field: surround modulation in primary visual cortex," The new visual neurosciences, pp. 425–444, 2013.

[18]. S. Shushruth, J. M. Ichida, J. B. Levitt, and A. Angelucci, "Comparison of spatial summation properties of neurons in macaque v1 and v2," Journal of neurophysiology, vol. 102, no. 4, pp. 2069–2083, 2009.

[19]. X.-S. Zhang, S.-B. Gao, C.-Y. Li, and Y.-J. Li, "A retina inspired model for enhancing visibility of hazy images," Frontiers in computational neuroscience, vol. 9, 2015.

[20]. S.-B. Gao, K.-F. Yang, C.-Y. Li, and Y.-J. Li, "Color constancy using double-opponency," IEEE transactions on pattern analysis and machine intelligence, vol. 37, no. 10, pp. 1973–1985, 2015.

[21]. U. D. Behrens and H. J. Wagner, "Adaptation-dependent changes of bipolar cell terminals in fish retina: effects on overall morphology and spinule formation in ma and mb cells," Vision Research, vol. 36, no. 24, pp. 3901–11, 1996.

[22]. K. He, J. Sun, and X. Tang, "Single image haze removal using dark channel prior," IEEE Transactions on Pattern Analysis and Machine Intelligence, vol. 33, no. 12, pp. 2341–2353, 2011.

[23]. Y.-T. Peng and P. C. Cosman, "Underwater image restoration based on image blurriness and light absorption," IEEE transactions on image processing, vol. 26, no. 4, pp. 1579–1594, 2017.

[24]. C. O. Ancuti, C. Ancuti, C. De Vleeschouwer, and P. Bekaert, "Color balance and fusion for underwater image enhancement," IEEE Transactions on Image Processing, vol. 27, no. 1, pp. 379– 393, 2018.

[25]. M. Babu Rao, Ch.Kavitha B. Prabhakara Rao, A.Govardhan, " Image Retrieval based on Local Histogram and texture features" is published International Journal of Computer science and information technologies vol.2 issue 2, March-April 2011.Published by Foundation of Computer Science, pp:741-746, ISSN:0975-5462, Impact factor:2.28

[26]. K.Kranthi Kumar, Kavitha Chaduvula, Babu Rao Markapudi, "A Detaied Survey on Feature Extraction Techniques In Image Processing for Medical Image Analysis", published in :European Journal of Molecular & Clinical" volume No:07 Issue No:10,2020,ISSN: 2525-825.